J. Biochem. **139**, 813–820 (2006)
doi:10.1093/jb/mvj099

The Intracellular Region of ClC-3 Chloride Channel Is in a Partially Folded State and a Monomer

Shu Jie Li[1,2,*], Masanobu Kawazaki[3], Kyoko Ogasahara[2] and Atsushi Nakagawa[2]

[1]Department of Biophysics, College of Physics Science, Nankai University, Tianjin 300071, P. R. China; [2]Institute for Protein Research, Osaka University, Osaka, 565-0871; and [3]Second Department of Internal Medicine, School of Medicine, Tokyo Medical and Dental University, Tokyo, 113

Received January 5, 2006; accepted February 15, 2006

In contrast to bacterial ClC chloride channels, all eukaryotic ClC chloride channels have a conserved long intracellular region that makes up of the carboxyl terminus of the protein and is necessary for channel functions as a channel gate. Little is known, however, about the molecular structure of the intracellular region of ClC chloride channels so far. Here, for the first time, we have expressed and purified the intracellular region of the rat ClC-3 chloride channel (C-ClC-3) as a water-soluble protein under physiological conditions, and investigated its structural characteristics and assembly behavior by means of circular dichroism (CD) spectroscopy, differential scanning calorimetry (DSC), size exclusion chromatography and analytical ultracentrifugation. The far-UV CD spectra of C-ClC-3 in the native state and in the presence of urea clearly show that the protein has a significantly folded secondary structure consisting of α-helices and β-sheets, while the near-UV CD spectra and DSC experiments indicate the protein is deficient in well-defined tertiary packing. Its Stokes radius is larger than its expected size as a folded globular protein, as determined on size exclusion chromatography. Furthermore, the DisEMBL program, a useful computational tool for the prediction of disordered/unstructured regions within a protein sequence, predicts that the protein is in a partially folded state. Based on these results, we conclude that C-ClC-3 is partially folded. On the other hand, both size exclusion chromatography and sedimentation equilibrium analysis show that C-ClC-3 exists as a monomer in solution, not a dimer like the whole ClC-3 molecule.

Key words: carboxyl terminus, ClC-3 chloride channel, expression, monomer, partially folded, purification.

Abbreviations: C-ClC-3, carboxyl terminus of ClC-3 chloride channel; IPTG, isopropyl-β-D-thiogalactopyranoside; PMSF, phenylmethylsulphonyl fluoride; EDTA, ethylenediamine tetraacetic acid; DTT, dithiothreitol; SDS-PAGE, sodium dodecyl sulfate–polyacrylamide gel electrophoresis; CD, circular dichroism.

Membrane protein ClC chloride channels widely found in both eukaryotic and prokaryotic cells form a large family. They play important roles in the regulation of cell volume (*1*, *2*), control of transepithelial transport (*3*), stabilization of membrane potential (*4*), and maintenance of intracellular pH (*5*).

As eukaryotic ClC chloride channels, *Torpedo* chloride channel ClC-0, and mammalian chloride channels ClC-1 to ClC-7, ClC-Ka and ClC-Kb have been identified (*6*). The muscle-type chloride channels, ClC-0 and ClC-1, are known to be responsible for the regulation of muscle excitability, and inactivation of these channels causes myotonia (*7–9*). The ubiquitously expressed ClC-2 and ClC-3 channels function as volume-activated chloride channels (*2*, *10*), but the volume-regulated function of ClC-3 remains controversial (*11*). ClC-4 generates strong outwardly rectifying chloride currents (*12*), but its physiological significance remains unclear. ClC-5 is involved in the acidification of renal endocytotic vesicles, which is necessary for proximal protein reabsorption, and the inactivation of which leads to kidney stones and dental disease (*13*, *14*). While the physiological role of ClC-6 remains unknown, ClC-7 is involved in HCl secretion, as demonstrated by the loss of ClC-7 chloride channel function in murine and human osteoclasts (*15*). ClC-Ka and ClC-Kb mediate transepithelial chloride transport in the kidney (*16*).

The topology of eukaryotic ClC chloride channels predicted on hydropathy analysis and supported by some experiments includes 13 relatively hydrophobic domains termed D1 to D13, which comprise 11 transmembrane-spanning domains, an extracellular domain (D4), and a carboxyl terminus region (D13) located on the cytoplasmic side of the membrane (*2*, *6*, *10*, *17*, *18*). In contrast to the bacterial proteins crystallized by Dutzler *et al*. (*19*), the long carboxyl terminal cytoplasmic stretch is conserved in eukaryotic ClC chloride channels, which contains two CBS (cystathionine beta synthase) domains (*20–23*) and may bind to other proteins (*24*). The studies have shown that the carboxyl terminus of ClC chloride channels is necessary for channel functions as a channel gate (*21–23*, *25*, *26–28*). Like the bacterial ClC proteins (*19*, *29*), the eukaryotic ClC chloride channels deduced on electrophysiological analysis of wild-type and mutant channels

*To whom correspondence should be addressed at: Institute for Protein Research, Osaka University, 3–2 Yamadaoka, Suita, Osaka 565-0871. Tel: +81-6-6879-8605, Fax: +81-6-6879-8606, E-mail: shujieli@protein.osaka-u.ac.jp

(*30*–*34*), and chemical cross-linking (*32*, *35*) also form a homodimeric architecture with two ion conduction pores formed by each single subunit (*33*, *34*).

The ClC-3 chloride channel was originally cloned from rat kidney and shows abundant expression in rat brain neuronal cells, mainly in the olfactory bulb, hippocampus, whose channel activity is regulated by protein kinase C (PKC), phorbol esters, and calcium/calmodulin-dependent protein kinase II (CaMKII) (*17*, *36*, *37*). The ClC-3 chloride channel, comprising 760 amino acid residues, is a volume-regulated chloride channel and necessary for the pH adjustment of several cell compartments (*2*, *5*). Although the overall amino acid sequence identities of ClC-3 with other ClC family members are very low, *e.g.*, 20.9% with ClC-0, 24% with ClC-1, and 26.3% with ClC-2, the topology of ClC-3 is the same as that of other ClC chloride channels (*6*, *17*), in which the last 181 amino acid residues located on the cytoplasmic side of the membrane comprise of its intracellular region (D13) (*2*).

To fully understand the electrophysiological characteristics of ClC chloride channels on a molecular basis, detailed structural information of the intracellular region of ClC chloride channels is necessary. Little is known yet, however, about its molecular structure and assembly characteristics. Does the intracellular region of ClC chloride channels have a folded structure? Do the two intracellular regions in a homodimeric ClC chloride channel also form a homodimer in the cytoplasm? To answer these questions, we have expressed and purified the intracellular region of rat ClC-3, and investigated its structural characteristics and assembly behavior by means of circular dichroism (CD) spectroscopy, circular dichroism (DSC), size exclusion chromatography and analytical ultracentrifugation. The results show that the intracellular region of ClC-3 is in a partially folded state and a monomer under physiological conditions. The biological implication of its hydrodynamic characteristics has also been discussed.

MATERIALS AND METHODS

Protein Expression—The gene that codes the intracellular region (residues 582–760) of rat ClC-3 was amplified by polymerase chain reaction (PCR) using ClC-3 cDNA containing in pSPORT 1(BRL) (*17*) as a template. The PCR product was cloned into the *Bam*HI and *Xho*I restriction endonuclease sites in the vector pGEX-6P-1 (Amersham Biosciences) as a fused protein with a glutathione S-transferase (GST) and preScission protease cleavage site for removal of the GST moiety. The cloned DNA was sequenced, and the expression plasmid, pGEX-C-ClC-3 was transformed into an *Escherichia coli* strain, BL21(DE3).

E. coli strain BL (DE3) cells carrying the expression plasmid pGEX-C-ClC-3 were grown at 21°C with shaking in Luria-Bertani medium supplemented with 100 μg/ml ampicillin. When the OD_{600} of the culture reached 1.0, IPTG was added to a final concentration of 0.5 mM to induce expression of the fused protein. After IPTG induction for 24 h at 14°C, cells were harvested by centrifugation at 5,000 × *g* for 10 min, and then washed with a buffer solution (50 mM sodium phosphate, 150 mM NaCl, pH 7.5).

Protein Purification—The washed cells were resuspended in lysis buffer (50 mM sodium phosphate buffer, pH 7.5, containing 0.5 M NaCl, 1.0 mM EDTA, 5 mM DTT, 0.2 mg/ml lysozyme, 1.0 mM PMSF, 3 μg/ml leupeptin and 3 μg/ml pepstatin A) at 4°C, and then disrupted by sonication on ice. Cell debris was removed by centrifugation at 150,000 × *g* for 30 min at 4°C, and the supernatant was loaded onto a Glutathione-Sepharose 4B (Amersham Bioscience) column equilibrated with the cleavage buffer (50 mM sodium phosphate buffer, pH 7.5, containing 0.5 M NaCl, 1 mM EDTA and 5 mM DTT) at 4°C. The column with bound C-ClC-3 was washed well with the cleavage buffer. To isolate C-ClC-3 from the GST moiety, preScission protease in the cleavage buffer was added to the column, and followed by incubation at 4°C for 16 h.

C-ClC-3 isolated from the GST moiety was eluted and concentrated to 5 mg/ml. The concentrated C-ClC-3 solution was then applied to a Superdex 200 16/60 gel filtration column (Amersham Biosciences) equilibrated with 20 mM sodium phosphate buffer, pH 7.5, containing 0.15 M NaCl, and eluted at a rate of 1.0 ml/min. The elution of C-ClC-3 was monitored as the absorption at 280 nm with an in-line detector (Amersham Bioscience). The fractions containing the protein, as judged on SDS-PAGE, were pooled and stored on ice. The concentration of the protein solution was determined by the method of Bradford using BSA as a standard (*38*).

SDS-PAGE and Western Blotting—SDS-PAGE was carried out on 12.5% (w/v) gels according to the method of Laemmli (*39*). Standard proteins (Bio-Rad) with a low molecular weight range were used to estimate protein molecular weights, and the gels were stained with Coomassie brilliant blue. Western blotting was performed with an anti–rClC-3 polyclonal antibody purchased from Alomone Laboratories (Jerusalem, Israel), which was raised in a rabbit against the rClC-3/GST fusion protein comprising residues 592–661 of rCLC-3 (*18*). The denatured proteins were separated by 12.5% SDS-PAGE and then transferred to a PVDF membrane (Amersham Biosciences) by semi-dry electroblotting. Nonspecific protein absorption was prevented using 5% (w/v) skim milk in phosphate-buffered saline containing 0.1% Tween 20 (PBS-T) for 1 h. Primary antibody incubation in PBS-T was performed for 1 h at room temperature. The HRP-coupled anti-rabbit secondary antibody (Amersham Biosciences) was used at a final dilution of 1/15,000 in PBS-T, and HRP was revealed with a chemiluminescent detection system (ECL+, Amersham Biosciences).

Circular Dichroism Spectroscopy—Far-UV (200–250 nm) and near-UV (250–350 nm) CD data were collected at 20°C with 0.1 nm intervals at the rate of 10 nm/min and a bandwidth of 1.0 nm by using two cuvettes: one with a light path-length of 1 mm for far-UV, and the other with a light path-length of 1 cm for near-UV on a Jasco-720 spectropolarimeter. The protein concentrations of samples were 0.5 mg/ml for far-UV and 2.0 mg/ml for near-UV in 20 mM sodium phosphate buffer (pH 7.5) containing 0.15 M NaCl and various concentrations of urea. The mean residue weight of 112.2 was used for calculation of the mean residue ellipticity. All CD spectra of the protein had the corresponding baseline spectra of the buffers used subtracted.

Differential Scanning Calorimetry—Differential scanning calorimetry (DSC) was performed with a high-sensitivity VP-DSC (Microcal Inc., USA) with a cell of

0.51 ml and at an excess pressure level of 30 psi to avoid degassing during heating at a protein concentration of 1.0 mg/ml. Both the buffer (20 mM sodium phosphate, pH 7.5, containing 0.15 M NaCl) and the protein sample were degassed by evacuation before measurements, and measured at a scanning rate of 1.0°C/min.

Size Exclusion Chromatography—Size exclusion chromatography was carried out on a gel filtration column Superdex 200 16/60 (Amersham Biosciences), monitored with on ÄKTAexplorer workstation (Amersham Biosciences) and equilibrated with equilibrium buffer (20 mM sodium phosphate buffer, pH 7.5, containing 0.15 M NaCl). One milliliter samples with various protein concentrations, from 1 to 5 mg/ml, were eluted at a flow rate of 1.0 ml/min. Elution profiles were monitored with an in-line UV-900 detector (Amersham Biosciences) at 280 nm. Peak fractions were analyzed by SDS-PAGE. The column was calibrated using proteins of known molecular weight and Stokes radus (Amersham Biosciences): ribonuclease A (13.7 kDa; 16.4 Å), chymotrypsinogen A (25.0 kDa; 20.9 Å), ovalbumin (43.0 kDa; 30.5 Å), bovine serum albumin (67.0 kDa; 35.5 Å), aldolase (158.0 kDa; 48.1 Å), catalase (232.0 kDa; 52.2 Å), ferritin (440.0 kDa; 61.0 Å), and thyroglobulin (669.0 kDa; 85.0 Å). The void volume was determined with Blue Dextran 2000. The partition coefficient, $K_{av} = (V_e - V_0)/(V_t - V_0)$, was calculated, where V_e, V_t and V_0 are the elution volumes of the protein samples, total bet volume and void volume, respectively. Two calibration curves for standard protein molecular weights and Stokes radii versus K_{av} were obtained, and the molecular weight and Stokes radius of C-ClC-3 were deduced from them.

Analytical Ultracentrifugation—C-ClC-3 was dialyzed overnight against 20 mM sodium phosphate buffer (pH 7.5) containing 0.15 M NaCl. The sample and dialysis buffer were loaded into Kel-F two-sector cells (cell length, 12 mm). Sedimentation equilibrium experiments were performed by using a Beckman Optima XL-A analytical ultracentrifugation in a Ti rotor at 18,000 rpm at 20°C. Sedimentation equilibrium data were collected at a wavelength of 275 nm with scans every 5 min. The partial specific volume calculated from the amino acid composition of C-ClC-3 was 0.7438. The sedimentation equilibrium data were analyzed using the XL-A data analysis software (Beckman, version 4.01).

Prediction of Intrinsic Disordered Regions—The disordered/unstructured regions within the C-ClC-3 sequence were predicted with the DisEMBL program, a useful computational tool for disordered regions within a protein sequence (*40*). The calculation conditions were as follows: the frames used were smooth = 8, peak = 8 and join = 4; the thresholds used were coils = 0.516, rem465 = 0.6 and hot loops = 0.1204; the temperature and pH were 5°C and 7.5, respectively.

RESULTS

Expression and Purification of C-ClC-3—In lysates of cells transformed with the expression plasmid after induction in a time-dependent manner, a specific band corresponding to a molecular weight of about 46 kDa, which corresponds to the molecular weight of C-ClC-3 fused with GST (46.5 kDa), was detected with the rClC-3 antibody (lines 3 and 4 in Fig. 1A). In contrast, the band was not observed for the lysate of cells transformed with the vector pGEX-6p-1 (line 1 in Fig. 1A). Coomassie-stained SDS-PAGE outlined the expression and purification stages of C-ClC-3 also showed that C-ClC-3 fused with GST was expressed well as a water-soluble protein (lines 2 and 3 in Fig. 1B). Furthermore, C-ClC-3 was successfully isolated from the GST moiety with protease, and was finally purified by gel filtration as a single band at a position corresponding to about 23.0 kDa (line 6 in Fig. 1B). The purified C-ClC-3 was also water-soluble in buffer solution.

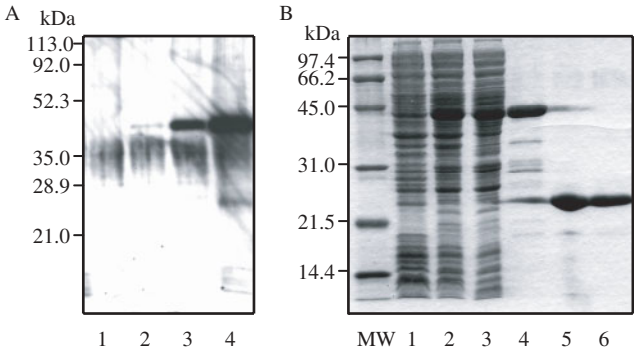

Fig. 1. **Expression and purification of C-ClC-3.** A: Western blotting of cell lysates before and after IPTG induction. Line 1, lysate of cells transformed with the vector pGEX-6P-1 as a control. Lines 2 to 4, lysates of cells transformed with the expression plasmid; line 2, cell lysate before induction; line 3, cell lysate after 12 h induction; line 4, cell lysate after 24 h induction. B: SDS-PAGE with Coomassie Brilliant Blue staining. MW shows the migration positions of standard proteins, with their molecular weights (in kDa) at the left. Line 1, cell lysate before induction; line 2, cell lysate after 24 h induction; line 3, supernatant of cell lysate after ultracentrifugation; line 4, C-ClC-3 fused with GST; line 5, C-ClC-3 isolated from the GST moiety with preScission protease; line 6, C-ClC-3 finally purified by gel filtration.

Analysis of the Secondary and Tertiary Structures of C-ClC-3—To determine whether the purified C-ClC-3 has a folded secondary structure, far-UV CD spectra of the protein in the native state and in the presence of various concentrations of urea were measured. As shown in Fig. 2A, the spectrum of the protein at 20°C in 20 mM sodium phosphate buffer (pH 7.5) containing 0.15 M NaCl showed a negative minimum around 207 nm and a shoulder around 222 nm, which indicated both α-helical and β-sheet contents (*41*, *42*). In the presence of urea, the negative CD values deceased and the shoulder around 222 nm gradually disappeared with an increase in the urea concentration, indicating that C-ClC-3 was denatured. The degree of denaturation of the protein was assessed by monitoring ellipticity changes at 222 nm as a function of the urea concentration. As shown in Fig. 2B, the unfolding of C-ClC-3 occurred at 1.5 M urea, the degree of the denaturation increased with the concentration of urea between 1.5 and 6 M, and a plateau above 6 M corresponded to complete denaturation.

As for the three-dimensional structure of C-ClC-3, near-UV CD spectra were obtained and DSC experiments were performed. The near-UV spectra in both native and completely denatured (6 M urea) states showed almost

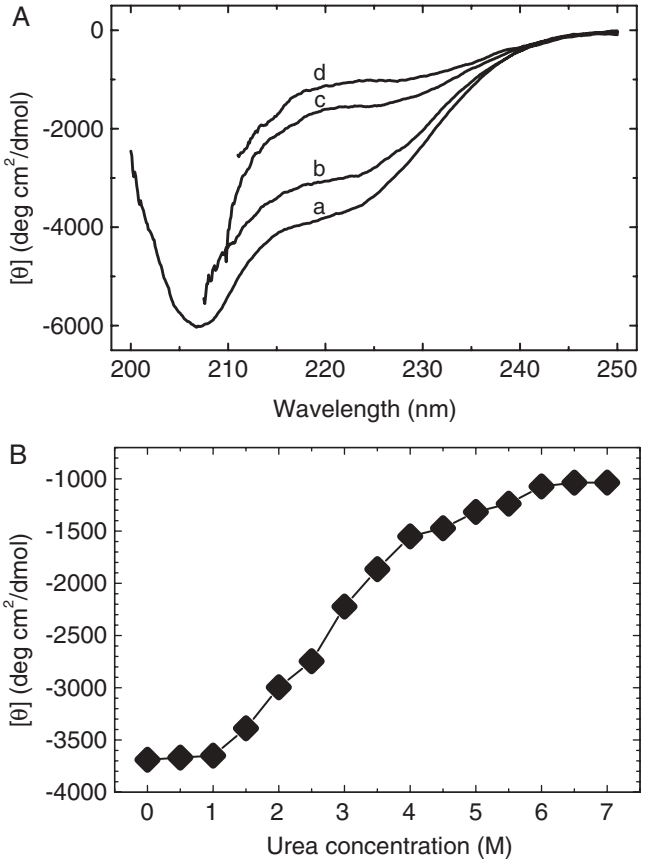

Fig. 2. **Far-UV CD spectra of C-ClC-3 in the native state and in the presence of urea.** CD spectra were obtained out at a protein concentration of 0.5 mg/ml at 20°C in 20 mM sodium phosphate buffer (pH 7.5) containing 0.15 M NaCl and various concentrations of urea. A, far-UV CD spectra of C-ClC-3 in 0 M (a), 2 M (b), 4 M (c) and 6 M urea (d), respectively. B, dependence of CD ellipticity at 222 nm on urea concentration.

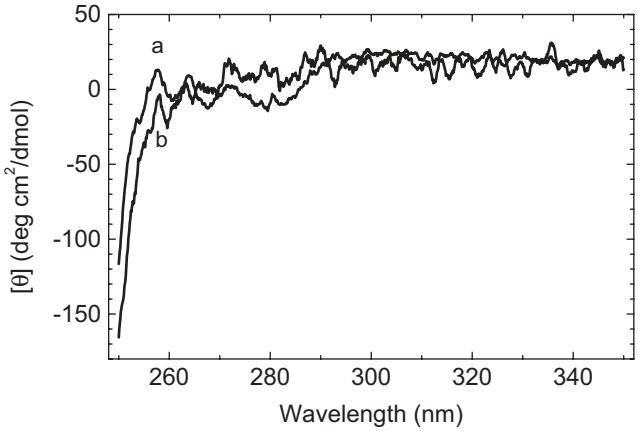

Fig. 3. **Near-UV CD spectra of C-ClC-3 in the native state (a) and in the fully unfolded state (b).** CD spectra were obtained at a protein concentration of 2.0 mg/ml at 20°C in 20 mM sodium phosphate buffer (pH 7.5) and 0.15 M NaCl containing 0 M urea (a) and 6 M urea (b), respectively.

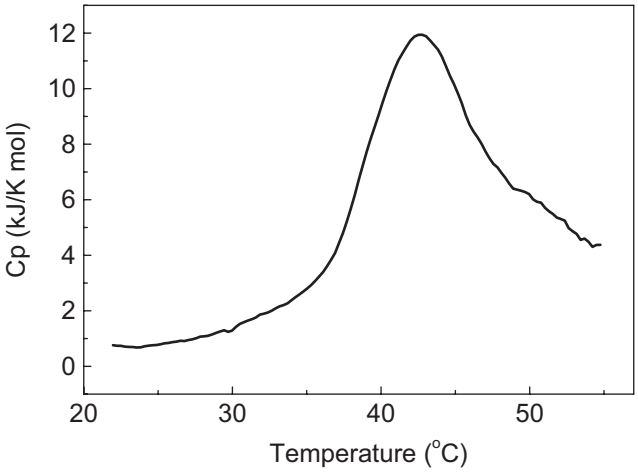

Fig. 4. **Excess heat capacity curve of C-ClC-3 in 20 mM sodium phosphate buffer (pH 7.5) containing 0.15 M NaCl at a protein concentration of 1.0 mg/ml.** The scanning rate was 1°C/min.

no significant signals originating from aromatic side chains (Fig. 3). Considering the fact that the protein contains no tryptophans and only one tyrosine, the near-UV spectra might not reflect its tertiary structure, in spite of that the spectra were measured at a high protein concentration (2 mg/ml). To measure its tertiary structure at high resolution, the DSC experiments were performed with a high-sensitive VP-DSC. The DSC curve of C-ClC-3 exhibited a peak of excess heat capacity at 42.5°C in 20 mM sodium phosphate buffer (pH 7.5) containing 0.15 M NaCl (Fig. 4). The heat denaturation of C-ClC-3 was irreversible, and the formation of amorphous aggregates could be observed with the naked eye after DSC experiments. The specific denaturation enthalpy change (Δh) of the protein, 4.1 J/g, was much lower than those of many folded globular proteins (between 10 and 27 J/g) (*43*). Therefore, we conclude that C-ClC-3 lacks well-defined tertiary packing.

Analysis of the Molecular Size and Assembly Behavior of C-ClC-3—The near-UV CD spectra and DSC study results revealed that C-ClC-3 lacks a compact tertiary structure. However, a significant secondary structure in C-ClC-3 observed in the far-UV CD studies strongly suggests that C-ClC-3 is in a partially folded state. Size exclusion chromatography is a useful method for estimating the hydrodynamic dimensions of a protein, and can elucidate the compactness of the protein's tertiary structure, because the Stokes radii of well-folded, partially or fully unfolded proteins are significant distinguishable. The Stokes radius of a protein in a partially folded state is larger than that in the fully folded state, and smaller than that in the fully unfolded state (*44–46*). As shown in Fig. 5A, only one sharp elution peak exhibiting high symmetry at a volume of 86.4 ml on the calibrated column on size exclusion chromatography was observed. The peak was close to the elution volume of the standard protein chymotrypsinogen A (25.0 kDa; 20.9 Å). This indicates that C-ClC-3 exists as a single species in solution. Figure 5, B and C, shows calibration curves, and the molecular weight and Stokes radius of C-ClC-3 deduced from them. The measured molecular weight and Stokes radius of C-ClC-3 were 28.6 kDa

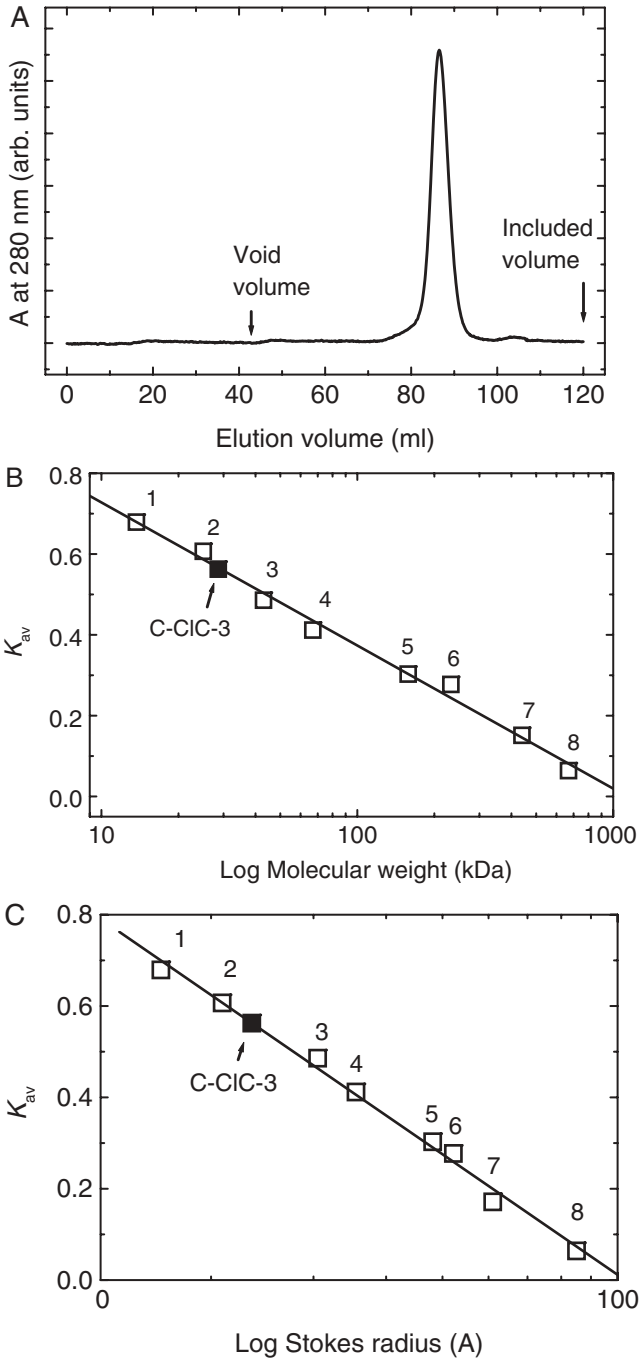

Fig. 5. **Size exclusion chromatography of C-ClC-3 on a Superdex 200 gel filtration column elution buffer, 20 mM sodium phosphate (pH 7.5) containing 0.15 M NaCl, at a flow rate of 1.0 ml/min and monitored at 280 nm.** A, elution profile as to the absorbance at 280 nm. B and C, calibration curves created from the molecular masses (B) and Stokes radii (C) of standards. The molecular masses and Stokes radii of the reference proteins were as follows: 1, ribonuclease A (13.7 kDa; 16.4 Å); 2, chymotrypsinogen A, (25.0 kDa; 20.9 Å); 3, ovalbumin (43.0 kDa; 30.5 Å); 4, bovine serum albumin (67.0 kDa; 35.5 Å); 5, aldolase (158.0 kDa; 48.1 Å); 6, catalase (232.0 kDa; 52.2 Å); 7, ferritin (440.0 kDa; 61.0 Å); and 8, thyroglobulin (669.0 kDa; 85.0 Å). The partition coefficient, K_{av}, is a function of the elution volumes of protein samples. The estimated molecular mass and Stokes radius of C-ClC-3 were 28.6 kDa and 23.5 Å, respectively. Open squares, reference proteins; solid squares, C-ClC-3.

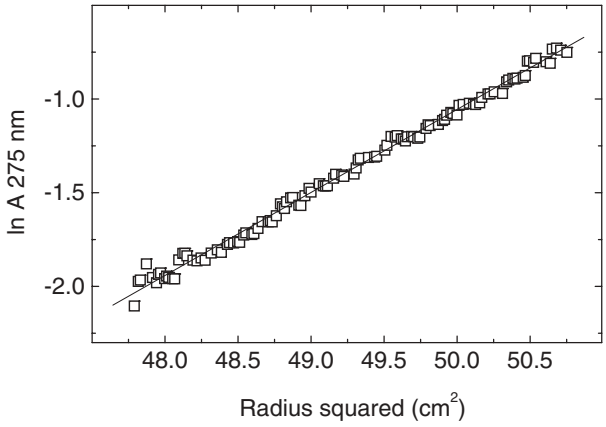

Fig. 6. **Analysis of the sedimentation equilibrium of C-ClC-3.** The sedimentation equilibrium experiment was performed at a protein concentration of 3.5 mg/ml in 20 mM sodium phosphate buffer (pH 7.5) containing 0.15 M NaCl at 20°C. The ln A_{275} *versus* the square of the radius from the axis of the rotation is plotted.

and 23.5 Å, respectively, which are larger than those of the monomer (20.5 kDa) but much smaller than those of the dimer (41.0 kDa) expected for a folded globular C-ClC-3 molecule. These results indicate that C-ClC-3 exists as a homogeneous monomer in solution, and has a larger Stokes radius, which arises from its loose tertiary structure.

All ClC chloride channels form a homodimer (*21*). The finding that C-ClC-3 could be a monomer is surprising. To further examine the assembly behavior of C-ClC-3, the sedimentation equilibrium method was employed with a protein concentration of 3.5 mg/ml. The dependence of absorbance at 275 nm on the radius-square well fitted a straight line at this protein concentration (Fig. 6). This means that there is a homogeneous molecular mass distribution of C-ClC-3 in solution, which is consistent with the results of size exclusion chromatography (Fig. 5). The measured molecular mass of C-ClC-3 was 21.6 kDa, which shows good agreement with its monomeric molecular weight of 20.5 kDa predicted from its amino acid sequence. This result also shows that C-ClC-3 remains a monomer, not a dimer like the whole ClC-3 molecule.

Prediction of Intrinsic Disordered Regions of C-ClC-3—To determine whether the amino acid sequence of C-ClC-3 has a partially folded propensity, the DisEMBL program, a useful computational tool for the prediction of disordered/unstructured regions within a protein sequence, was used, which is highly accurate, predicting more than 60% of hot loops with <2% false positives (*40*). The results predicted with DisEMBL are summarized in Table 1, which also indicates that C-ClC-3 is in a partially folded state, as shown on differential scanning calorimetry (DSC) and size exclusion chromatography. On the other hand, the GlobPlot program was also used to predict the disordered regions of C-ClC-3 (*47*), which clearly predicted that there are two CBS domains and some disordered regions in C-ClC-3. Because GlobPlot is less accurate than DisEMBL in coil prediction, and was designed as a visual inspection tool for finding domain boundaries, repeats and unstructured regions, and the GlobPlot algorithm is very simple and intuitive, as described by the authors of GlobPlot (*40*).

Table 1. **Prediction of the disordered regions of C-ClC-3 with DisEMBL.**

Loops	1–9, 14–40, 46–62, 84–129, 168–179
Hotloops	1–25, 79–89, 97–110, 168–179
REM465	82–91

Here we only showed the results predicted with the DisEMBL program.

DISCUSSION

It is well established that proteins can exist in three different states, *i.e.*, fully unfolded, partially folded and completely folded forms (*47*). The partially folded state of proteins can be defined as the persistence of a secondary structure but without a compact tertiary structure, and is observed in the presence of denaturants (*46*, *48*). The following four physical quantities determined in the above experiments indicate that C-ClC-3 is in a partially folded state: (i) significant contents of helical and sheet secondary structure, (ii) no compact tertiary structure, (iii) a larger Stokes radius compared with folded globular C-ClC-3, and (iv) a disordered propensity predicted with the DisEMBL program.

More than 100 intrinsically disordered/unstructured proteins are known (*49–51*), including Tau (*52*), Prions (*53*), and partially p53 (*54*). Although little is known about the cellular and structural meaning of this state, it may become ordered when on binding to another molecule (*55*). The intrinsically disordered/unstructured proteins may play a central role in diseases through protein misfolding and aggregation (*56*). That C-ClCl-3 is in a partially folded state in solution might be interpreted in two ways. One possibility is that there are no tryptophans in the protein, which are known to be important for protein structural stability (*46*). Another possibility is the lack of the corresponding transmembrane domains that interact with the intracellular region. The several truncations of the carboxyl terminus of ClC-0 were mainly expressed in inclusion bodies (*27*), implying that the carboxyl terminus of ClC-0 is unstable and indirectly supporting our conclusion.

We used two different techniques to assess the assembly behavior of C-ClC-3: size exclusion chromatography and sedimentation equilibrium analysis. Both techniques lead to the conclusion that C-ClC-3 forms a monomer, not a dimer like the whole ClC-3 molecule (*32–34*). The assembly behavior is stable between pH 5–8 and up to 1.5 M sodium chloride (data not shown), as confirmed by CD spectra and size exclusion chromatography (data not shown). Co-expression experiments on the heterodimeric channel constructed with different carboxyl terminus proteins suggested that each intracellular region of ClC-1 folds independently and that there are not interactions between them (*28*), while analyses of its intracellular region functions indicated that the intracellular region in ClC-1 may not be needed for dimerization (*22*). Therefore, it can be deduced that, in general, the two intracellular regions in homodimeric ClC chloride channels comprise a monomer not a dimer.

The functional significance of the carboxyl terminus of ClC chloride channels is mainly illustrated by various mutations and truncations of both ClC-0 and ClC-1 (*22*, *26–28*). When the carboxyl terminus of ClC-0 is deleted, the chloride current becomes un-observable (*27*). The normal function of the ClC-1 protein also depends on the integrity of the intracellular region (*25*, *26*). Moreover, Hebeisen *et al*. (*28*) showed that only the wild type is functional in heterodimeric channels of ClC-1 consisting of one wild type subunit and one subunit completely devoid of its intracellular region. This result indicates that the intracellular region of ClC-1 independently supports the channel functions of ClC-1 in a single subunit. The eukaryotic ClC chloride channels have two ion pores formed by each subunit individually in dimeric ClC channels (*33*, *34*). Our present work and other recent studies on ClC-1 (*22*, *28*) may indicate that in the double-barreled architecture of ClC channels, each intracellular region acts only on each corresponding chloride-conduction pore, and that the role of the intracellular region, as an essential functional region involved intimately in the gating of ClC chloride channels, is independently functional in the two channel halves.

Authors are deeply grateful to Prof. Tomitake Tsukihara, Institute for Protein Research, Osaka University, for supporting and encouraging the research and helpful discussion on the manuscript. Authors thank Mrs. Miyo Sakai of Institute for Protein Research, Osaka University, for her excellent technical assistant for analytical ultracentrifugation experiments.

REFERENCES

1. Worrell, R.T., Butt, A.G., Cliff, W.H., and Frizzel, R.A. (1989) A volume-sensitive chloride conductance in human colonic cell line T84. *Am. J. Physiol.* **256**, C1111–C1119
2. Duan, D., Winter, C., Cowley, S., Hume, J.R., and Horowitz, B. (1997) Molecular identification of a volume-regulated chloride channel. *Nature* **390**, 417–421
3. McCann, J.D. and Welsh, M.J. (1990) Regulation of Cl^- and K^+ channels in airway epithelium. *Annu. Rew. Physiol.* **52**, 115–135
4. Steinmeyer, K., Ortland, C., and Jentsch, T.J. (1991) Primary structure and functional expression of a developmentally regulated skeletal muscle chloride channel. *Nature* **354**, 301–304
5. Li, X., Wang, T., Zhao, Z., and Weinman, S.A. (2002) The CLC-3 chloride channel promotes acidification of lysosomes in CHO-K1 and Huh-7 cells. *Am. J. Physiol. Cell Physiol.* **282**, C1483-C1491
6. Jentsch, T.J. (1996) Chloride channels: a molecular perspective. *Curr. Opin. Neurobiol.* **6**, 303–310
7. Jentsch, T.J., Steinmeyer, K., and Schwarz, G. (1990) Primary structure of *Torpedo marmorata* chloride channel isolated by expression cloning in Xenopus oocytes. *Nature* **348**, 510–514
8. Steinmeyer, K., Lorenz, C., Pusch, M., Koch, M.C., and Jentsch, T.J. (1994) Multimeric structure of ClC-1 chloride channel revealed by mutations in dominant myotonia congenital. *EMBO J.* **13**, 37–743
9. Meyer-Kleine, C., Steinmeyer, K., Ricker, K., Jentsch, T.J., and Koch, M.C. (1995) Spectrum of mutations in the mayor human skeletal muscle chloride channel gene (ClCN1) leading to myotonia. *Am. J. Hum. Genet.* **57**, 1325–1334
10. Gründer, S., Thiemann, A., Pusch, M., and Jentsch, T.J. (1992) Regions involved in the opening of ClC-2 chloride channel by voltage and cell volume. *Nature* **360**, 759–762

11. Weylandt, K.H., Valverde, M.A., Nobles, M., Raguz, S., Amey, J.S. Diaz, M., Nastrucci, C., Higgins, C.F., and Sardini, A. (2001) Human ClC-3 is not the swelling-activated chloride channel involved in cell volume regulation. *J. Biol. Chem.* **276**, 17461–17467
12. Friedrich, T., Breiderhoff, T., and Jentsch, T.J. (1999) Mutational analysis demonstrates that ClC-4 and ClC-5 directly mediate plasma membrane currents. *J. Biol. Chem.* **274**, 896–902
13. Lloyd, S.E., Pearce, S.H.S., Fisher, S.E., Steinmeyer, K., Schwappach, B., Scheinman, S.J., Harding, B., Bolino, M., Devoto, M., Goodyer, P., Redgen, S.P.A., Wrong, O., Jentsch, T.J., Craig, I.W., and Thakker, R.V. (1996) A common molecular basis of three inherited kidney stone diseases. *Nature* **379**, 445–449
14. Günther, W., Luchow, A., Cluzeaud, F., Vandewalle, A., and Jentsch, T.J. (1998) ClC-5, the chloride channel mutated in Dent's disease, colocalizes with the proton pump in endocytotically active kidney cells. *Proc. Natl. Acad. Sci. USA* **95**, 8075–8080
15. Kornak, U., Kasper, D., Bösl, M.R, Kaiser, E., Schweizer, M., Schulz, A., Friedrich, W., Delling, G., and Jentsch, T.J. (2001) Loss of the ClC-7 chloride channel leads to osteopetrosis in mice and man. *Cell* **104**, 205–215
16. Kieferle, S., Fong, P., Bens, M., Vandewalle, A., and Jentsch, T.J. (1994) Two highly homologous members of the CLC chloride channel family in both rat and human kidney. *Proc. Natl. Acad. Sci. USA* **91**, 6943–6947
17. Kawasaki, M., Uchida, S., Monkawa, T., Miyawaki, A., Mikoshiba, K., Marumo, F., and Sasaki, S. (1994) Cloning and expression of a protein kinase C-regulated chloride channel abundantly expressed in rat brain neuronal cells. *Neuron* **12**, 597–604
18. Schmieder, S., Lindenthal, S., and Ehrenfeld, J. (2001) Tissue-specific N-glycosylation of the CLC-3 chloride channel. *Biochem. Biophys. Res. Commun.* **286**, 635–640
19. Dutzler, R., Campbell, E.B., Cadene, M., Chait, B.T., and MacKinnon, R. (2002) X-ray structure of a ClC chloride channel at 3.0 Å reveals the molecular basis of anion selectivity. *Nature* **415**, 287–294
20. Schmidt-Rose, T. and Jentsch, T.J. (1997) Transmembrane topology of a CLC chloride channel. *Proc. Natl. Acad. Sci. UAS* **94**, 7633–7638
21. Estévez, R. and Jentsch, T.J. (2002) CLC chloride channels: correlating structure and function. *Curr. Opin. Struct. Biol.* **12**, 531–539
22. Estévez, R., Pusch, M., Ferrer-Costa, C., Orozco, M., and Jentsch, T.J. (2004) Functional and structural conservation of CBS domains from CLC chloride channels. *J. Physiol.* **557**, 363–378
23. Carr, G., Simmons, N., and Sayer, J. (2005) A role for CBS domain 2 in trafficking of chloride channel CLC-5. *Biochem. Biophys. Res. Commun.* **310**, 600–605
24. Schwake, M., Friedrich, T., and Jentsch, T.J. (2001) An internalization signal in ClC-5, an endosomal Cl-channel mutated in dent's disease. *J. Biol. Chem.* **276**, 12049–12054
25. Schmidt-Rose, T. and Jentsch, T.J. (1997) Reconstitution of functional voltage-gated chloride channels from complementary fragments of CLC-1. *J. Biol. Chem.* **272**, 20515–20521
26. Hryciw, D.H., Rychkov, G.Y., Hughes, B.P., and Bretag, A.H. (1998) Relevance of the D13 region to the function of the skeletal muscle chloride channel. *J. Biol. Chem.* **273**, 4304–4307
27. Maduke, M., Williams, C., and Miller, C. (1998) Formation of CLC-0 chloride channels from separated transmembrane and cytoplasmic domains. *Biochemistry* **37**, 1315–1321
28. Hebeisen, S., Biela, A., Giese, B., Muller-Newen, G., Hidalgo, P., and Fahlke, C. (2004) The role of the carboxyl terminus in ClC chloride channel function. *J. Biol. Chem.* **279**, 3140–13147
29. Maduke, M., Pheasant, D.J., and Miller, C. (1999) High-level expression, functional reconstitution, and quaternary structure of a prokaryotic ClC-type chloride channel. *J. Gen. Physiol.* **114**, 713–722
30. Miller, C. and White, M.M. (1984) Dimeric structure of single chloride channels from *Torpedo* electroplax. *Proc. Natl. Acad. Sci. USA* **81**, 2772–2775
31. Bauer, C.K., Steinmeyer, K., Schwarz, J.R., and Jentsch, T.J. (1991) Completely functional double-barrelled chloride channel expressed from a single *Torpedo* cDNA. *Proc. Natl. Acad. Sci. USA* **88**, 11052–11056
32. Middleton, R.E., Pheasant, D.J., and Miller, C. (1994) Purification, reconstitution, and subunit composition of a voltage-gated chloride channel from *Torpedo* electroplax. *Biochemistry* **33**, 13189–13198
33. Middleton, R.E., Pheasant, D.J., and Miller, C. (1996) Homodimeric architecture of a ClC-type chloride ion channel. *Nature* **383**, 337–340
34. Ludewig, U., Pusch, M., and Jentsch, T.J. (1996) Two physically distinct pores in the dimeric ClC-0 chloride channel. *Nature* **383**, 340–343
35. Fahlke, C., Knittle, T., Gurnett, C.A., Campbell, K.P., and George, A.L. Jr. (1997) Subunit stoichiometry of human muscle chloride channels. *J. Gen. Physiol.* **109**, 93–104
36. Kawasaki, M., Suzuki, M., Uchida, S., Sasaki, S., and Marumo, F. (1995) Stable and functional expression of the ClC-3 chloride channel in somatic cell lines. *Neuron* **14**, 1285–1291
37. Huang, P., Liu, J., Di, A., Robinson, N.C., Musch, M.W., Kaetzel, M.A., and Nelson, D.J. (2001) Regulation of human CLC-3 channels by multifunctional Ca^{2+}/calmodulin-dependent protein kinase. *J. Biol Chem.* **276**, 20093–20100
38. Bradford, M.M. (1976) A rapid and sensitive method for the quantitation of microgram quantities of protein utilizing the principle of protein-dye binding. *Anal. Biochem.* **72**, 248–254
39. Laemmli, U.K. (1970) Cleavage of structural protein during the assembly of the head of bacteriophage T_4. *Nature* **227**, 680–685
40. Linding, R., Jensen, L.J., Diella, F., Bork, P., Gibson, T.J., and Russell, R.B. (2003) Protein disorder prediction: implications for structural proteomics. *Structure* **11**, 1453–1459
41. Manavalan, P. and Johnson, W.C.Jr. (1983) Sensitivity of circular dichroism to protein tertiary structure class. *Nature* **305**, 831–832
42. Johnson, W.C. Jr. (1988) Secondary structure of proteins through circular dichroism spectroscopy. *Ann. Rev. Biophys. Biophys. Chem.* **17**, 145–166
43. Privalov, P.L. and Gill, S.J. (1988) Stability of protein structure and hydrophobic interaction. *Adv. Protein Chem.* **39**, 191–234
44. Kuznetsova, I.M., Stepanenko, O.V., Turoverov, K.K., Zhu, L., Zhou, J.M., Fink, A.L., and Uversky, V.N. (2002) Unraveling multistate unfolding of rabbit muscle creatine kinase. *Biochim. Biophys. Acta* **1596**, 138–155
45. Uversky, V.N. (1993) Use of fast protein size-exclusion liquid chromatography to study the unfolding of proteins which denature through the molten globule. *Biochemistry* **32**, 13288–13298
46. Perraut, C., Clottes, E., Leydier, C., Vial, C., and Marcillat, O. (1998) Role of quaternary structure in muscle creatine kinase stability: tryptophan 210 is important for dimer cohesion. *Proteins* **32**, 43–51
47. Linding, R., Russell, R.B., Neduva, V., and Gibson, T.J. (2003) GlobPlot: Exploring protein sequences for globularity and disorder. *Nucleic Acids Res.* **31**, 3701–3708
48. Semisotnov, G.V., Rodionova, N.A., Razgulyaev, O.I., Uversky, V.N., Gripas', A.F., and Gilmanshin, R.I. (1991) Study of the "molten globule" intermediate state in protein folding by a hydrophobic fluorescent probe. *Biopolymers* **31**, 119–128

49. Dyson, H.J. and Wright, P.E. (2002) Coupling of folding and binding for unstructured proteins. *Curr. Opin. Struct. Biol.* **12**, 54–60
50. Wright, P.E. and Dyson, H.J. (1999) Intrinsically unstructured proteins: re-assessing the protein structure-function paradigm. *J. Mol. Biol.* **293**, 321–331
51. Tompa, P. (2002) Intrinsically unstructured proteins. *Trends Biochem. Sci.* **27**, 527–533
52. Schweers, O., Schonbrunn-Hanebeck, E., Marx, A., and Mandelkow, E. (1994) Structural studies of tau protein and Alzheimer paired helical filaments show no evidence for beta-structure. *J. Biol. Chem.* **269**, 24290–24297
53. Gossert, A.D., Bonjour, S., Lysek, D.A., Fiorito, F., and Wuthrich, K. (2005) Prion protein NMR structures of elk and of mouse/elk hybrids. *Proc. Natl. Acad. Sci. USA* **102**, 646–650
54. Kussie, P.H., Gorina, S., Marechal, V., Elenbaas, B., Moreau, J., Levine, A.J., and Pavletich, N.P. (1996) Structure of the MDM2 oncoprotein bound to the p53 tumor suppressor transactivation domain. *Science* **274**, 948–953
55. Uversky, V.N. (2002) Natively unfolded proteins: a point where biology waits for physics. *Protein Sci.* **11**, 739–756
56. Dunker, A.K., Brown, C.J., Lawson, J.D., Iakoucheva, L.M., and Obradovic, Z. (2002) Intrinsic disorder and protein function. *Biochemistry* **41**, 6573–6582